Published in final edited form as:
Hepatology. 2009 December ; 50(6): 1861–1870. doi:10.1002/hep.23214.

Sorafenib Inhibits Signal Transducer and Activator of Transcription-3 Signaling in Cholangiocarcinoma Cells by Activating the Phosphatase Shatterproof 2

Boris R. A. Blechacz[1], **Rory L. Smoot**[1], **Steven F. Bronk**[1], **Nathan W. Werneburg**[1], **Alphonse E. Sirica**[2], and **Gregory J. Gores**[1]

[1]Miles and Shirley Fiterman Center for Digestive Diseases, Division of Gastroenterology and Hepatology, College of Medicine, Mayo Clinic, Rochester, MN

[2]Department of Pathology, Division of Cellular and Molecular Pathogenesis, Virginia Commonwealth University School of Medicine, Richmond, VA

Abstract

The Janus kinase/signal transducer and activator of transcription (JAK/STAT) pathway is one of the key signaling cascades in cholangiocarcinoma (CCA) cells, mediating their resistance to apoptosis. Our aim was to ascertain if sorafenib, a multikinase inhibitor, may also inhibit JAK/STAT signaling and, therefore, be efficacious for CCA. Sorafenib treatment of three human CCA cell lines resulted in Tyr^{705} phospho-STAT3 dephosphorylation. Similar results were obtained with the Raf-kinase inhibitor ZM336372, suggesting sorafenib promotes Tyr^{705} phospho-STAT3 dephosphorylation by inhibiting Raf-kinase activity. Sorafenib treatment enhanced an activating phosphorylation of the phosphatase SHP2. Consistent with this observation, small interfering RNA–mediated knockdown of phosphatase shatterproof 2 (SHP2) inhibited sorafenib-induced Tyr^{705} phospho-STAT3 dephosphorylation. Sorafenib treatment also decreased the expression of Mcl-1 messenger RNA and protein, a STAT3 transcriptional target, as well as sensitizing CCA cells to tumor necrosis factor–related apoptosis-inducing ligand (TRAIL)-mediated apoptosis. In an orthotopic, syngeneic CCA model in rats, sorafenib displayed significant tumor suppression resulting in a survival benefit for treated animals. In this *in vivo* model, sorafenib also decreased tumor Tyr^{705} STAT3 phosphorylation and increased tumor cell apoptosis.

Conclusion—Sorafenib accelerates STAT3 dephosphorylation by stimulating phosphatase SHP2 activity, sensitizes CCA cells to TRAIL-mediated apoptosis, and is therapeutic in a syngeneic rat, orthotopic CCA model that mimics human disease.

Cholangiocarcinoma (CCA) is the most common biliary malignancy. Unfortunately, its incidence is increasing in several Western countries.[1] Therapeutic options for CCA are limited, and the overall prognosis for patients with CCA is dismal, with median survival being less than 24 months. New insights into the biology of this cancer may provide a framework for targeted therapeutic approaches. CCA, similar to hepatocellular carcinoma and colorectal cancer, often arises in an inflammatory environment.[2,3] Inflammation-associated carcinogenesis is, in part,

Correspondence to: Gregory J. Gores.

Address reprint requests to: Gregory J. Gores, M.D., College of Medicine, Mayo Clinic, 200 First Street SW, Rochester, MN 55905. gores.gregory@mayo.edu; fax: 507-284-0762.

Potential conflict of interest: Nothing to report.

Additional Supporting Information may be found in the online version of this article.

mediated by dysregulated cytokine signaling pathways,4 which potentially can be therapeutically targeted for treatment of this cancer.

Members of the signal transducers and activators of transcription (STAT) family are key signal transducers in cytokine and growth factor signaling. Especially STAT3 has been shown to be an essential signaling molecule in carcinogenesis through its transcriptional activity on genes regulating apoptosis, proliferation, differentiation, and angiogenesis.5,6 One of the main activators of STAT3 in CCA cells is interleukin-6 (IL-6) via Janus kinases (JAK).7 IL-6 is a cytokine secreted by inflammatory cells (i.e., macrophages) but also by CCA cells where it activates STAT3 by autocrine and paracrine mechanisms.2,3,8,9 Under physiologic conditions, the JAK/STAT3 signaling pathway is tightly regulated through negative feedback mechanisms including protein phosphatases.7 In CCA, IL-6–mediated JAK/STAT3 signaling was found to be dysregulated due to epigenetic silencing of suppressor of cytokine signaling-3.[10] Interestingly, interruption of JAK/STAT3 signaling either through JAK inhibitors or STAT3 small interfering RNA (siRNA) resulted in sensitization to tumor necrosis factor–related apoptosis-inducing ligand (TRAIL)-mediated apoptosis through down-regulation of the STAT3 transcriptional target Mcl-1, an antiapoptotic Bcl-2 family protein.[8]

Sorafenib was developed as a c-Raf kinase inhibitor, although it also targets several other Raf-kinases (wild-type b-Raf, b-Raf V600) as well as other receptor tyrosine kinases.[11] Sorafenib prolongs survival of patients with hepatocellular carcinoma.12 Recently, inhibition of STAT3 phosphorylation by sorafenib was observed in medulloblastoma and esophageal carcinoma. 13,14 These studies were predominantly observational, and the mechanisms by which sorafenib inhibits STAT3 phosphorylation were not elucidated. Given this information, the effect of sorafenib on STAT3 regulation in CCA warrants exploration as a potential therapeutic agent.

The objective of this study was to examine the effect of sorafenib on the JAK/STAT3 signaling cascade in CCA cells. The results of this study suggest that sorafenib inhibits the JAK/STAT3 signaling axis at the level of STAT3 phosphorylation, resulting in down-regulation of Mcl-1, thereby sensitizing human CCA cells to TRAIL-mediated apoptosis. The inactivation of phospho-STAT3 occurs by a phosphatase shatterproof 2 (SHP2)-dependent mechanism which appears to be stimulated by Raf-kinase inhibition. Furthermore, in an orthotopic, syngeneic rodent CCA model, sorafenib achieves significant tumor suppression.

Materials and Methods

Cell Lines and Culture

The human CCA cell lines HuCCT-1,15 KMCH-1,16 Mz-ChA-1,17 and TFK-118 were cultured in Dulbecco's modified Eagle medium (DMEM) supplemented with 10% fetal bovine serum, penicillin G (100 U/mL), streptomycin (100 μg/mL), and gentamicin (100 μg/mL) as described.[9] The erythroblastic leukemia viral oncogene homolog (ErbB2)-transformed malignant rat cholangiocyte cell line BDEneu was cultured in DMEM supplemented with 10% fetal bovine serum, insulin (0.1 μmol/L), transferrin (5 μg/mL), penicillin G (100 U/mL), streptomycin (100 μg/mL), and G418 (500 μg/mL) under standard conditions as described. 19,20

Quantitation of Apoptosis

Apoptosis in cell culture was quantified by assessing the characteristic nuclear changes of apoptosis after staining with 4′,6-diamidino2-phenylindole dihydrochloride (DAPI; Sigma Chemicals, St. Louis, MO) using fluorescence microscopy.21 Caspase-3/7 activity was quantitated using the ApoONE Homogenous Caspase-3/7 Assay (Promega, Madison, WI)

according to manufacturer's recommendations.21 Apoptosis in paraffin-embedded tissue sections was quantified using a fluorescent terminal deoxynucleotidyl transferase-mediated dUTP nick-end labeling (TUNEL) assay (Roche, Mannheim, Germany) as previously described.22

Real-Time Polymerase Chain Reaction for Mcl-1

Total RNA was extracted from the cells using the Trizol Reagent (Invitrogen), and was reverse-transcribed into complementary DNA with Moloney leukemia virus reverse transcriptase and random primers (Invitrogen). Quantification of the complementary Mcl-1 DNA template was performed with real-time polymerase chain reaction (LightCycler; Roche Molecular Biochemicals, Mannheim, Germany) using SYBR green (Molecular Probes) as previously described by us in detail.[8]

Immunoblot Analysis

Proteins from whole-cell lysates were analyzed by immunoblot analysis; whole-cell lysates were prepared as previously described.10 Proteins were separated by sodium dodecyl sulfate polyacrylamide gel electrophoresis (SDS-PAGE) followed by transfer to nitrocellulose membrane as previously described by us in detail.[10] Proteins were visualized using enhanced chemiluminescence (ECL) reagents (Amersham Biosciences) and Kodak X-OMAT film.

Phosphatase Silencing

Phosphatases SHP1, SHP2, and PTPRT were knocked down using commercially available siRNA(Qiagen, Valencia, CA). Cells were transfected using siPORT Lipid (Ambion, Austin, TX). Briefly, cells were plated at 30% density. The next day, the cells were transfected in Opti-MEM with 30 nM siRNA using siPORT reagent according to the manufacturer's recommendations. Medium was added 4 hours after transfection, and the cells were then incubated for 60 hours at 37°C. Knockdown was confirmed by immunoblot analysis.

Cellular Localization of STAT3

Cells were grown on coverslips and fixed with phosphate-buffered saline (PBS) (pH 7.4) containing 4% paraformaldehyde at 4°C for 15 minutes. After washing in PBS three times (each for 5 minutes), the cells were permeabilized in PBS containing 0.1% Triton X-100 at room temperature for 15 minutes. The cells were washed again in PBS three times (each for 5 minutes) and blocked in blocking buffer (PBS containing 3% bovine serum albumin) at room temperature for 60 minutes. Next, the cells were then incubated with anti-STAT3 polyclonal antibody at a dilution of 1:1500 in the blocking buffer at 4°C overnight, washed in PBS three times (each for 5 minutes), and incubated with cyanine 3-conjugated goat anti-rabbit immunoglobulin G (Jackson ImmunoResearch, West Grove, PA) at a dilution of 1:1500 in the blocking buffer at room temperature for an additional 60 minutes. The subcellular distribution of STAT3 was analyzed by confocal microscope (Zeiss LSM S10; Carl Zeiss, Thornwood, NJ).

Tyr^{705}-Phospho STAT3 in Tissue

Immunohistochemistry for Tyr^{705} phospho-STAT3 on paraffin-embedded BDEneu tumors was performed as previously described.[10] Briefly, tumor samples were deparaffinized in xylene, hydrated with graded ethanol and distilled water, followed by heat-induced antigen-retrieval in Tris/ethylene diamine tetraacetic acid (pH 9.0). Immunohistochemical staining was performed employing the DakoCytomation EnVision+ System HRP (DAB) (DakoCytomation, Carpinteria, CA) according to the manufacturer's recommendations.

Animal Experiments

All animal studies were performed in accordance with and approved by the Institutional Animal Care and Use Committee. In vivo cell transplantation was carried out in adult Fischer 344 male rats (Harlan, Indianapolis, IN) with initial mean body weights between 200 and 220 g. Animals were anesthetized by administration of 90 mg/kg ketamine and 10 mg/kg xylazine intraperitoneally. Below the sternum, a small longitudinal incision (5–10 mm) was made in order to expose the common bile duct. The left hepatic duct was identified and ligated using sterile, nonabsorbable 5–0 silk surgical suture material. BDE-neu cells suspended in 0.1 mL sterile PBS were injected into the parenchyma of the corresponding left hepatic lobe followed by closure of the laparotomy wound by suturing of fasciae and skin using simple intermittent and running sutures using absorbable 6-0 coated vicryl suture material.

Materials, IL-6 Quantitation, and Statistical Analysis

Materials, quantitation of IL-6 secretion, and statistical analysis are provided in the Supporting Information.

Results

Sorafenib Results in Tyr^{705} STAT3 Dephosphorylation

The predominant pathway for STAT3 Tyr^{705}-phosphorylation is JAK-mediated.[5] However, Tyr^{705}-phosphorylation of STAT3 through other pathways such as Src, MEK-kinase 1 and EGFR have been described in certain cell types.[23,24] Therefore, we confirmed JAK as the main Tyr^{705}-phosphorylation pathway for STAT3 in HuCCT-1 cells. Neither treatment with Src-inhibitors, EGFR-inhibitors, nor ERK1/2-inhibitors at doses of onefold to 1000-fold of their median inhibitory concentration (IC_{50}) inhibited Tyr^{705}-phosphorylation of STAT3 in HuCCT-1 cells (Fig. 1A). In CCA cells, IL-6 is one of the main JAK/STAT3 pathway activators.[8,10] Therefore, we next examined if sorafenib alters IL-6 secretion by HuCCT-1 cells. Sorafenib did not decrease IL-6 secretion into the media (3.6 ± 0.76 pg/μL with vehicle versus 4.8 ± 0.43 pg/μL with sorafenib) (Fig. 1B). Next, we assessed the effect of sorafenib on expression of the IL-6 receptor complex including gp80, gp130, and JAK1 and JAK2.[7] Treatment with sorafenib did not inhibit or decrease expression of gp80, gp130, JAK1, or JAK2 (Fig. 1B). Likewise, activation of the IL-6 receptor, as indicated by autophosphorylation of JAK1, JAK2 and phosphorylation of gp130, was also not inhibited by sorafenib (Fig. 1B). In contrast, sorafenib treatment decreased Tyr^{705}-phosphorylated STAT3 without altering total STAT3 protein levels (Fig. 1C). This dephosphorylation of STAT3 was sustained over 12 hours indicating a robust, nontransient mechanism for reducing the Tyr^{705}-phosphorylated form of this transcription factor. Sorafenib induced Tyr^{705} phospho-STAT3 dephosphorylation was also confirmed in two other CCA cell lines, KMCH-1 and Mz-Cha-1 (Fig. 1D).

Because sorafenib inhibits Raf-kinases, we next ascertained if inhibition of Raf-kinases also induces Tyr^{705} phospho-STAT3 dephosphorylation. Cells were treated with two different concentrations of the Raf-kinase inhibitor ZM336372, resulting in dose-dependent inhibition of c-Raf and b-Raf, respectively.[25] Both concentrations resulted in dephosphorylation of Tyr^{705} phospho-STAT3 (Fig. 1E). These data implicate Raf-inhibition as a potential mediator of sorafenib-induced Tyr^{705} STAT3-dephosphorylation.

Tyr^{705}-phosphorylation of STAT3 is required for its nuclear accumulation, and thereby its transcriptional activity for antiapoptotic proteins such as Mcl-1.[7,8] Immunofluorescence demonstrated STAT3 to be predominantly localized to the nuclear compartment of untreated cells. In contrast, sorafenib treatment resulted in an inhibition of nuclear STAT3 accumulation, resulting in its predominantly cytoplasmic localization (Fig. 2A,B). Finally, to confirm the functional inactivation of the JAK/STAT3 pathway, we examined expression of Mcl-1 in

sorafenib-treated HuCCT-1 cells. Sorafenib treatment caused a reduction in both Mcl-1 mRNA and protein levels (Fig. 2C,D). Taken together, these data further demonstrate that sorafenib disrupts the STAT3 signaling pathway in CCA cell lines.

Sorafenib-Induced Tyr^{705} STAT3 Dephosphorylation Is Mediated by Phosphatase SHP2

JAK/STAT3 signaling is tightly regulated through negative feedback mechanisms involving phosphatases which may directly dephosphorylate STAT3.[26,27] Candidate phosphatases responsible for these inactivating mechanisms include PTPRT, SHP1, SHP2 and TC45.[26–31] Treatment of HuCCT-1 cells with sorafenib plus the nonspecific phosphatase inhibitor sodium-pervanadate (25–200 nM) resulted in a dose-dependent inhibition of the sorafenib-mediated Tyr^{705} STAT3 dephosphorylation (Fig. 3A). Sodium pervanadate also blocked Tyr^{705} STAT3 dephosphorylation by the Raf-kinase inhibitor ZM336372 (Fig. 3B). Also, cellular levels ofMcl-1, a transcriptional target of Tyr^{705} phospho-STAT3, are preserved by cotreatment with sodium pervanadate (Fig. 3C). These observations suggest that sorafenib induces dephosphorylation of STAT3 by stimulating phosphatase activity.

To identify which of these candidate phosphatases mediate sorafenib-induced Tyr^{705} STAT3 dephosphorylation, silencing of the corresponding phosphatases was performed using siRNA technology. No effect on sorafenib-induced Tyr^{705} STAT3 dephosphorylation was observed despite effective knockdown of phosphatase SHP1 and PTPRT (data not shown). However, knockdown of SHP2 resulted in abrogation of sorafenib stimulated Tyr^{705} STAT3 dephosphorylation (Fig. 4A). The activation of phosphatase SHP2 by sorafenib was further confirmed by immunoblot analysis for the activated form of SHP2, Tyr^{580} phospho-SHP2. Treatment of HuCCT-1 cells with 1 μM and 10 μM sorafenib resulted in a 1.66-fold and 1.82-fold increase in Tyr^{580} phospho-SHP2 (Fig. 4B). Thus, sorafenib treatment of HuCCT-1 cells results in Tyr^{705} STAT3 dephosphorylation by stimulation of SHP2 activity.

Sorafenib Sensitizes CCA Cells to Apoptosis

To evaluate the potential anti-neoplastic effect of sorafenib on cholangiocarcinoma cells in vitro, the cytotoxic effects of sorafenib monotherapy and combined sorafenib-TRAIL treatment were examined. As assessed either by morphologic criteria or caspase-3/7 activity, neither sorafenib nor TRAIL monotherapy induced significant apoptosis in HuCCT-1 and KMCH-1 cells. In contrast, the combination was associated with significant apoptosis induction (Fig. 5A,B). These observations are consistent with our prior data indicating that disruption of STAT3 signaling with loss of Mcl-1 expression sensitizes CCA cells to TRAIL cytotoxicity.[8] The sorafenib-mediated sensitization of the human CCA cell lines HuCCT-1 and KMCH-1 was dosedependent (Fig. 5C). However, silencing of phosphatase SHP2 resulted in significant attenuation of the sorafenib-induced sensitization to TRAIL in comparison to untransfected ($P < 0.05$) and scramble siRNA transfected HuCCT-1 cells ($P < 0.05$) (Fig. 5D). These data support phosphatase SHP2 as a key mediator of sorafenib-induced sensitization to TRAIL cytotoxicity.

As previously reported,[18] sorafenib monotherapy induced apoptosis in TFK-1 cells as confirmed by morphologic analysis as well as capase-3/7 assay (Fig. 6A). Similar to the other human CCA cell lines, sorafenib treatment also resulted in a marked decrease in Tyr^{705} p-STAT3 (Fig. 6B). Thus, dependent on the CCA cell line' sorafenib either induces apoptosis or sensitizes CCA cells to TRAIL-mediated apoptosis.

Sorafenib Is Tumor Suppressive in a Rodent CCA Model

To ascertain if the cytotoxic effects of sorafenib on CCA observed *in vitro* are translatable to an *in vivo* model, we employed an established syngeneic, orthotopic rat model of CCA.[19,20] One week after tumor cell implantation and left hepatic duct ligation, treatment was initiated

with sorafenib at a dose of 10 mg/kg body weight/day, a dose equivalent to the dose currently in use in humans with hepatocellular carcinoma.[12] Therapy was initiated 7 days after tumor implantation and given for 7 days. After 1 week of treatment, therapy was discontinued and animals analyzed 21 days after tumor implantation. Macroscopic analysis confirmed extensive tumor growth in vehicle-treated, BDEneu cell–injected animals (Fig. 7A). However, treatment with sorafenib resulted in significant tumor suppression with complete tumor regression in 22% of the treatment group. Untreated animals showed a significant increase in their tumor-to-body weight ratio secondary to hepatic carcinomatosis. However, in sorafenib-treated animals this ratio was at control values (Fig. 7A). At the time of tumor analysis (21 days after tumor implantation), extensive tumor growth had resulted in death of all vehicle-treated animals. In comparison, 60% of sorafenib-treated animals were still alive at the same time point (Fig. 7B). Immunohistochemical evaluation of BDEneu tumors for Tyr^{705} phospho STAT3, displayed tumor nuclear staining in vehicle-treated animals (Fig. 7C). However, in sorafenib-treated animals, nuclear Tyr^{705} phospho-STAT3 immunoreactivity was virtually absent. This Tyr^{705} STAT3 dephosphorylation in BDEneu tumors was associated with increased tumor cell apoptosis (Fig. 7D). Minimal apoptosis was observed in nontumorous hepatic tissue, confirming the tumor specificity of the sorafenib-mediated sensitization of CCA cells to apoptosis (Fig. 7D). Thus, sorafenib is tumor suppressive in this rodent model of CCA.

Discussion

The results of this study provide new insights regarding the potential efficacy of sorafenib for the treatment of CCA. These data indicate that sorafenib: (1) inhibits the JAK/STAT3 signaling axis by stimulating net Tyr^{705} STAT3 dephosphorylation which is associated with Mcl-1 down-regulation and sensitization to TRAIL-induced apoptosis; (2) mediates Tyr^{705} STAT3 dephosphorylation by a phosphatase SHP2-dependent pathway; and (3) results in tumor suppression in an orthotopic, syngeneic rodent model of CCA. Each of these observations is discussed in detail below.

Our data suggest sorafenib inhibits the JAK/STAT3 signaling pathway by stimulating Tyr^{705} dephosphorylation of STAT3. At the time of finalizing our studies, three publications also reported an effect of sorafenib and sunitinib in reducing cellular levels of Tyr^{705} phospho-STAT3 in esophageal cancer, renal cell carcinoma and medulloblastoma cells.[13,14,32] Our results, however, extend these studies by identifying the mechanism for sorafenib associated Tyr^{705}-dephosphorylation of STAT3. Our current observations indicate that phosphatase inhibition by sodium-pervanadate completely abrogates the sorafenib-induced decrease of Tyr^{705} phospho-STAT3. These results implicate phosphatase activation by sorafenib as a mechanism of Tyr^{705} STAT3 dephosphorylation. Sorafenib stimulated phosphatase SHP2 activation was identified by its Tyr^{580} activating phosphorylation. Furthermore, siRNA targeted knockdown of phosphatase SHP2 resulted in abrogation of the sorafenib mediated effect on Tyr^{705} phospho-STAT3. Based on these observations SHP2 is likely the phosphatase responsible for sorafenib-induced Tyr^{705} STAT3 dephosphorylation. These data are consistent with prior studies indicating that Tyr^{705} phospho-STAT3 is a direct substrate of SHP2.[27] Our studies also suggest that the sorafenib-induced Tyr^{705} STAT3 dephosphorylation is mediated by Raf inhibition, a known sorafenib target, as the Raf-inhibitor ZM336372 also results in Tyr^{705} STAT3 dephosphorylation. For example, concentrations of ZM336372 which are selective for c-Raf inhibition also results in dephosphorylation of Tyr^{705} STAT3. Taken together, our results suggest sorafenib induces Tyr^{705} dephosphorylation of STAT3 by inhibiting Raf which results in enhanced phosphatase SHP2 activity.

Huether et al. observed apoptosis *in vitro* with sorafenib monotherapy in two CCA cell lines.[18] Our data confirm apoptosis following sorafenib monotherapy of TFK-1 cells, one of the cell lines used by Huether et al. However, in none of the other human CCA cell lines evaluated in

our study did sorafenib monotherapy induce apoptosis. The difference between cell lines in regards to apoptosis induction by sorafenib is likely due to variation in the dependence of the cell lines on STAT3 activation for survival.[4,33]

We observed significant sensitization to TRAIL induced apoptosis with sorafenib in several human CCA cell lines. Because sorafenib reduced cellular Mcl-1 levels, these findings are consistent with our previous observations that down-regulation of this antiapoptotic Bcl-2 protein sensitizes CCA cells to TRAIL cytotoxicity.[8,34] Other mechanisms of sorafenib-induced down-regulation of Mcl-1 have been reported which can enhance or complement STAT3 inactivation including alterations in NF-κB–mediated transcription, inhibition of eIF4E-associated translation, and accelerated proteosomal degradation.[34–38] Loss of cellular Mcl-1 by sorafenib by these multiple mechanisms should help ensure a pharmacologic effect on this molecular target and contribute to either single agent or combination therapy.

Sorafenib displayed significant CCA tumor suppression in our *in vivo* CCA model. A syngeneic, orthotopic rodent model of CCA was employed for these studies. Not only does this model reflect a similar molecular signature as human CCA,[20] but the syngeneic, orthotopic model avoids the problems of immunocompromise and incompatibilities of the tumor microenvironment problematic in human xenograft models. In contrast to the *in vitro* studies, increased levels of apoptosis were observed in the BDE tumors of sorafenib-treated animals. Previously, we reported that CCA cells produce TRAIL upon stimulation with interferon-γ, a likely component of the inflammatory microenvironment.[39] Sorafenib-mediated Mcl-1 down-regulation in CCA cells may result in their sensitization to an endogenous TRAIL autocrine-mediated and/or paracrine-mediated cytotoxic pathway. This concept may explain the complete tumor regression in one-fifth of animals treated with sorafenib. Our results suggest sorafenib warrants further evaluation for the treatment of human CCA.

Supplementary Material

Refer to Web version on PubMed Central for supplementary material.

Abbreviations

CCA	cholangiocarcinoma
DAPI	4′ ,6-diamidino-2-phenylindole dihydrochloride
IL-6	interleukin-6
JAK	Janus kinase
PBS	phosphate-buffered saline
SDS-PAGE	sodium dodecyl sulfate polyacrylamide gel electrophoresis
siRNA	small interfering RNA
STAT	signal transducer and activator of transcription
TRAIL	tumor necrosis factor–related apoptosis-inducing ligand

Acknowledgments

This work was supported by a grant from the National Institutes of Health (NIH) DK59427 (G.J.G.), NIH R01 CA 83650, R01 CA 39225 (A.E.S.), the Mayo Clinic Clinical Investigator Program (B.R.A.B.), the optical microscopy core from NIH DK84567 and the Mayo Foundation.

References

1. Blechacz B, Gores GJ. Cholangiocarcinoma: advances in pathogenesis, diagnosis, and treatment. Hepatology 2008;48:308–321. [PubMed: 18536057]
2. Bollrath J, Phesse TJ, von Burstin VA, Putoczki T, Bennecke M, Bateman T, et al. gp130-mediated Stat3 activation in enterocytes regulates cell survival and cell-cycle progression during colitis-associated tumorigenesis. Cancer Cell 2009;15:91–102. [PubMed: 19185844]
3. Grivennikov S, Karin E, Terzic J, Mucida D, Yu GY, Vallabhapurapu S, et al. IL-6 and Stat3 are required for survival of intestinal epithelial cells and development of colitis-associated cancer. Cancer Cell 2009;15:103–113. [PubMed: 19185845]
4. Yu H, Jove R. The STATs of cancer–new molecular targets come of age. Nat Rev Cancer 2004;4:97–105. [PubMed: 14964307]
5. Aggarwal BB, Sethi G, Ahn KS, Sandur SK, Pandey MK, Kunnumakkara AB, et al. Targeting signal-transducer-and-activator-of-transcription-3 for prevention and therapy of cancer: modern target but ancient solution. Ann N Y Acad Sci 2006;1091:151–169. [PubMed: 17341611]
6. Hirano T, Ishihara K, Hibi M. Roles of STAT3 in mediating the cell growth, differentiation and survival signals relayed through the IL-6 family of cytokine receptors. Oncogene 2000;19:2548–2556. [PubMed: 10851053]
7. Heinrich PC, Behrmann I, Haan S, Hermanns HM, Muller-Newen G, Schaper F. Principles of interleukin (IL)-6-type cytokine signalling and its regulation. Biochem J 2003;374:1–20. [PubMed: 12773095]
8. Isomoto H, Kobayashi S, Werneburg NW, Bronk SF, Guicciardi ME, Frank DA, et al. Interleukin 6 upregulates myeloid cell leukemia-1 expression through a STAT3 pathway in cholangiocarcinoma cells. Hepatology 2005;42:1329–1338. [PubMed: 16317687]
9. Kobayashi S, Werneburg NW, Bronk SF, Kaufmann SH, Gores GJ. Interleukin-6 contributes to Mcl-1 up-regulation and TRAIL resistance via an Akt-signaling pathway in cholangiocarcinoma cells. Gastroenterology 2005;128:2054–2065. [PubMed: 15940637]
10. Isomoto H, Mott JL, Kobayashi S, Werneburg NW, Bronk SF, Haan S, et al. Sustained IL-6/STAT-3 signaling in cholangiocarcinoma cells due to SOCS-3 epigenetic silencing. Gastroenterology 2007;132:384–396. [PubMed: 17241887]
11. Wilhelm SM, Adnane L, Newell P, Villanueva A, Llovet JM, Lynch M. Preclinical overview of sorafenib, a multikinase inhibitor that targets both Raf and VEGF and PDGF receptor tyrosine kinase signaling. Mol Cancer Ther 2008;7:3129–3140. [PubMed: 18852116]
12. Llovet JM, Ricci S, Mazzaferro V, Hilgard P, Gane E, Blanc JF, et al. Sorafenib in advanced hepatocellular carcinoma. N Engl J Med 2008;359:378–390. [PubMed: 18650514]
13. Delgado JS, Mustafi R, Yee J, Cerda S, Chumsangsri A, Dougherty U, et al. Sorafenib triggers antiproliferative and pro-apoptotic signals in human esophageal adenocarcinoma cells. Dig Dis Sci 2008;53:3055–3064. [PubMed: 18512153]
14. Yang F, Van Meter TE, Buettner R, Hedvat M, Liang W, Kowolik CM, et al. Sorafenib inhibits signal transducer and activator of transcription 3 signaling associated with growth arrest and apoptosis of medulloblastomas. Mol Cancer Ther 2008;7:3519–3526. [PubMed: 19001435]
15. Miyagiwa M, Ichida T, Tokiwa T, Sato J, Sasaki H. A new human cholangiocellular carcinoma cell line (HuCC-T1) producing carbohydrate antigen 19/9 in serum-free medium. In Vitro Cell Dev Biol 1989;25:503–510. [PubMed: 2544546]
16. Murakami T, Yano H, Maruiwa M, Sugihara S, Kojiro M. Establishment and characterization of a human combined hepatocholangiocarcinoma cell line and its heterologous transplantation in nude mice. Hepatology 1987;7:551–556. [PubMed: 3032760]
17. Knuth A, Gabbert H, Dippold W, Klein O, Sachsse W, Bitter-Suermann D, et al. Biliary adenocarcinoma. Characterisation of three new human tumor cell lines. J Hepatol 1985;1:579–596. [PubMed: 4056357]
18. Huether A, Hopfner M, Baradari V, Schuppan D, Scherubl H. Sorafenib alone or as combination therapy for growth control of cholangiocarcinoma. Biochem Pharmacol 2007;73:1308–1317. [PubMed: 17266941]

19. Lai GH, Zhang Z, Shen XN, Ward DJ, Dewitt JL, Holt SE, et al. erbB-2/neu transformed rat cholangiocytes recapitulate key cellular and molecular features of human bile duct cancer. Gastroenterology 2005;129:2047–2057. [PubMed: 16344070]
20. Sirica AE, Zhang Z, Lai GH, Asano T, Shen XN, Ward DJ, et al. A novel “patient-like” model of cholangiocarcinoma progression based on bile duct inoculation of tumorigenic rat cholangiocyte cell lines. Hepatology 2008;47:1178–1190. [PubMed: 18081149]
21. Malhi H, Barreyro FJ, Isomoto H, Bronk SF, Gores GJ. Free fatty acids sensitise hepatocytes to TRAIL mediated cytotoxicity. Gut 2007;56:1124–1131. [PubMed: 17470478]
22. Kahraman A, Barreyro FJ, Bronk SF, Werneburg NW, Mott JL, Akazawa Y, et al. TRAIL mediates liver injury by the innate immune system in the bile duct-ligated mouse. Hepatology 2008;47:1317–1330. [PubMed: 18220275]
23. Schaefer LK, Wang S, Schaefer TS. c-Src activates the DNA binding and transcriptional activity of Stat3 molecules: serine 727 is not required for transcriptional activation under certain circumstances. Biochem Biophys Res Commun 1999;266:481–487. [PubMed: 10600528]
24. Lim CP, Cao X. Regulation of Stat3 activation by MEK kinase 1. J Biol Chem 2001;276:21004–21011. [PubMed: 11278353]
25. Hall-Jackson CA, Eyers PA, Cohen P, Goedert M, Boyle FT, Hewitt N, et al. Paradoxical activation of Raf by a novel Raf inhibitor. Chem Biol 1999;6:559–568. [PubMed: 10421767]
26. Lehmann U, Schmitz J, Weissenbach M, Sobota RM, Hortner M, Friederichs K, et al. SHP2 and SOCS3 contribute to Tyr-759-dependent attenuation of interleukin-6 signaling through gp130. J Biol Chem 2003;278:661–671. [PubMed: 12403768]
27. Gunaje JJ, Bhat GJ. Involvement of tyrosine phosphatase PTP1D in the inhibition of interleukin-6-induced Stat3 signaling by alpha-thrombin. Biochem Biophys Res Commun 2001;288:252–257. [PubMed: 11594781]
28. Ahn KS, Sethi G, Sung B, Goel A, Ralhan R, Aggarwal BB. Guggulsterone, a farnesoid X receptor antagonist, inhibits constitutive and inducible STAT3 activation through induction of a protein tyrosine phosphatase SHP-1. Cancer Res 2008;68:4406–4415. [PubMed: 18519703]
29. Han Y, Amin HM, Franko B, Frantz C, Shi X, Lai R. Loss of SHP1 enhances JAK3/STAT3 signaling and decreases proteosome degradation of JAK3 and NPM-ALK in ALK+ anaplastic large-cell lymphoma. Blood 2006;108:2796–2803. [PubMed: 16825495]
30. ten Hoeve J, de Jesus Ibarra-Sanchez M, Fu Y, Zhu W, Tremblay M, David M, et al. Identification of a nuclear Stat1 protein tyrosine phosphatase. Mol Cell Biol 2002;22:5662–5668. [PubMed: 12138178]
31. Zhang X, Guo A, Yu J, Possemato A, Chen Y, Zheng W, et al. Identification of STAT3 as a substrate of receptor protein tyrosine phosphatase T. Proc Natl Acad Sci USA 2007;104:4060–4064. [PubMed: 17360477]
32. Xin H, Zhang C, Herrmann A, Du Y, Figlin R, Yu H. Sunitinib inhibition of Stat3 induces renal cell carcinoma tumor cell apoptosis and reduces immunosuppressive cells. Cancer Res 2009;69:2506–2513. [PubMed: 19244102]
33. Darnell JE. Validating Stat3 in cancer therapy. Nat Med 2005;11:595–596. [PubMed: 15937466]
34. Dai Y, Grant S. Targeting multiple arms of the apoptotic regulatory machinery. Cancer Res 2007;67:2908–2911. [PubMed: 17409392]
35. Kim SH, Ricci MS, El-Deiry WS. Mcl-1: a gateway to TRAIL sensitization. Cancer Res 2008;68:2062–2064. [PubMed: 18381408]
36. Rahmani M, Davis EM, Bauer C, Dent P, Grant S. Apoptosis induced by the kinase inhibitor BAY 43-9006 in human leukemia cells involves down-regulation of Mcl-1 through inhibition of translation. J Biol Chem 2005;280:35217–35227. [PubMed: 16109713]
37. Ricci MS, Kim SH, Ogi K, Plastaras JP, Ling J, Wang W, et al. Reduction of TRAIL-induced Mcl-1 and cIAP2 by c-Myc or sorafenib sensitizes resistant human cancer cells to TRAIL-induced death. Cancer Cell 2007;12:66–80. [PubMed: 17613437]
38. Yu C, Bruzek LM, Meng XW, Gores GJ, Carter CA, Kaufmann SH, et al. The role of Mcl-1 downregulation in the proapoptotic activity of the multikinase inhibitor BAY 43-9006. Oncogene 2005;24:6861–6869. [PubMed: 16007148]

39. Ishimura N, Isomoto H, Bronk SF, Gores GJ. Trail induces cell migration and invasion in apoptosis-resistant cholangiocarcinoma cells. Am J Physiol Gastrointest Liver Physiol 2006;290:G129–G136. [PubMed: 16166346]

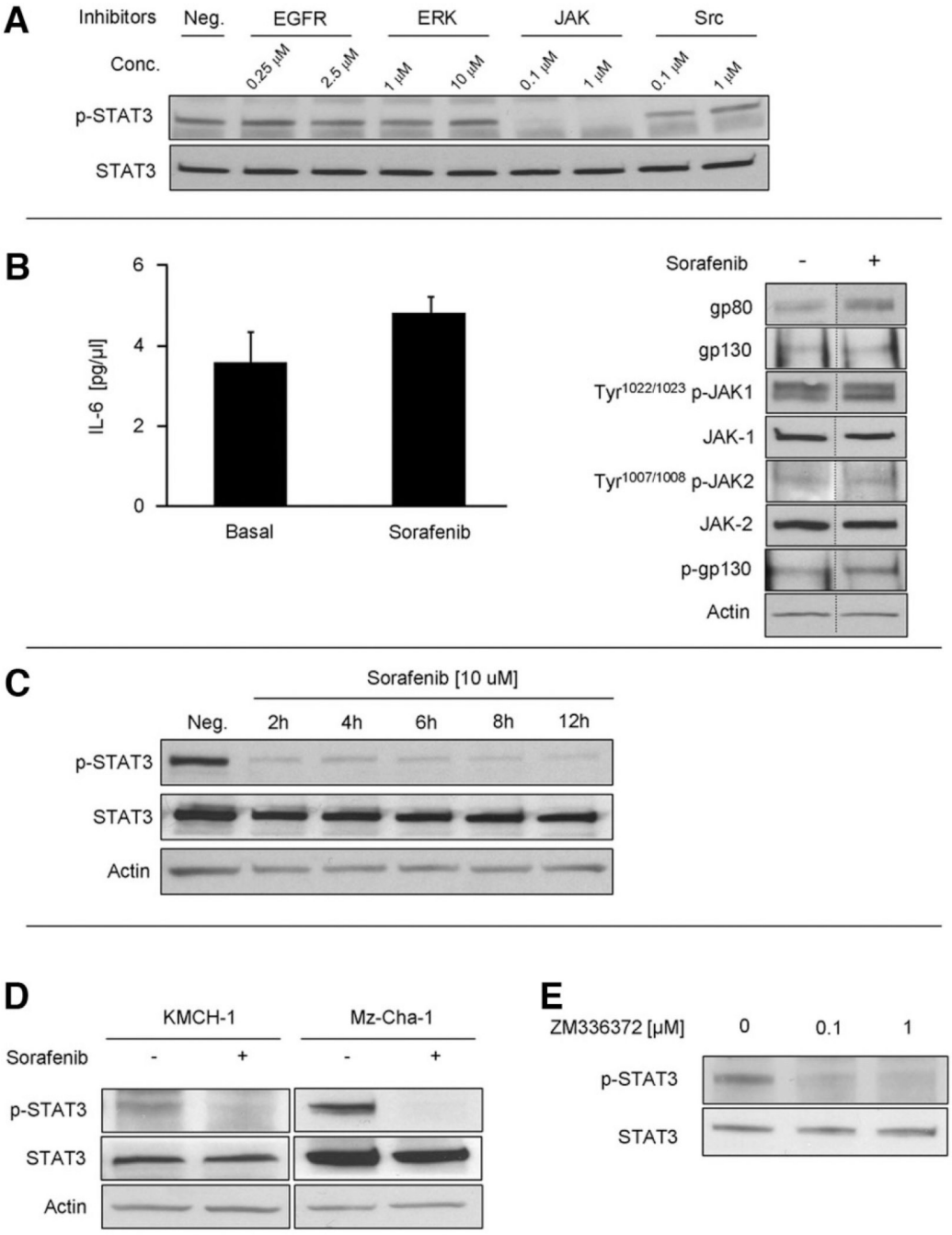

Fig. 1.

Sorafenib interferes with IL-6 signaling by loss of Tyr^{705} phospho-STAT3. HuCCT-1 cells were treated in the presence or absence of sorafenib (10 μM) for 12 hours. (A) Inhibition of known STAT3 activating signaling pathways. HuCCT-1 cells were treated with JAK-1/2, ERK-1/2, Src and EGFR inhibitors at the indicated doses for 4 hours followed by immunoblot analysis of whole-cell lysates for Tyr^{705} phospho-STAT3. (B) Effect of sorafenib on IL-6 secretion (left panel) and on the IL-6 receptor complex (right panel). IL-6 secretion by HuCCT-1 cells into the supernatant was quantified by enzyme-linked immunosorbent assay. The IL-6 receptor complex was evaluated by SDS-PAGE and immunoblot analysis of protein (50 μg) obtained from whole-cell lysates. Bands were cut and combined (separated by dotted

line) from the same radiograph. (C) Immunoblot analysis of sorafenib on total and Tyr^{705} phospho-STAT3 in HuCCT-1 cells. (D) Immunoblot analysis of sorafenib on total and Tyr^{705} phospho-STAT3 in KMCH-1 and Mz-Cha-1 cells. (E) Immunoblot analysis of the Raf-inhibitor ZM336372 on total and Tyr^{705} phospho-STAT3 in HuCCT-1 cells.

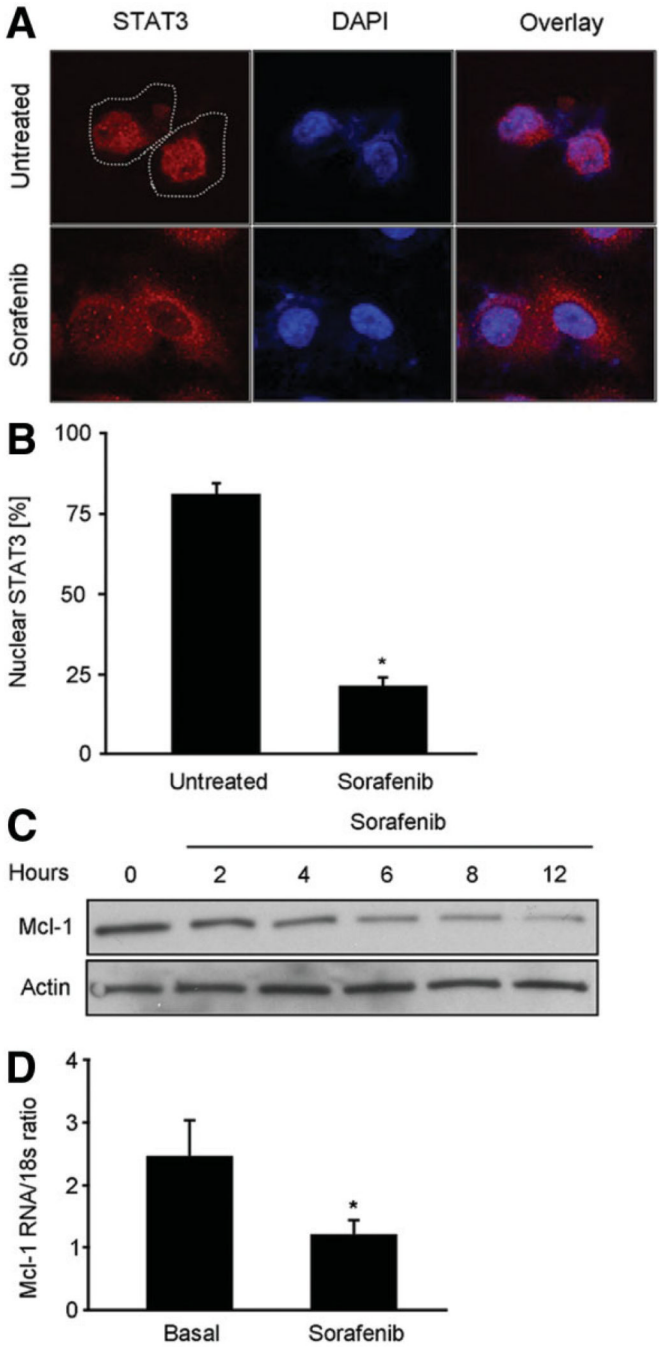

Fig. 2.

Sorafenib inhibits transcriptional activity of STAT3 and results in loss of cellular Mcl-1. HuCCT-1 cells were treated with sorafenib (10 μM) followed by analysis of STAT3 cellular localization and Mcl-1 expression. (A) Sorafenib-treated and untreated cells were subjected to immunocytochemistry for anti-STAT3 antibody and analyzed by confocal microscopy. DAPI staining and overlay demonstrate nuclear accumulation of STAT3 in untreated, but not in sorafenib-treated cells. (B) Percentages of cells with nuclear STAT3 fluorescence were quantitated by imaging total nuclei labeled with DAPI (10 μg/mL). (C) Immunoblot analysis for Mcl-1 protein expression. As assessed by immunoblot analysis, Mcl-1 protein levels decreased as early as 2 hours following sorafenib treatment. (D) Quantitative real-time

polymerase chain reaction for Mcl-1 mRNA. Cellular RNA was isolated from sorafenib-treated and untreated cells 2 hours after treatment, and analyzed for Mcl-1 mRNA as described in Materials and Methods section. Note the significant reduction ($P < 0.05$) in Mcl-1 mRNA levels.

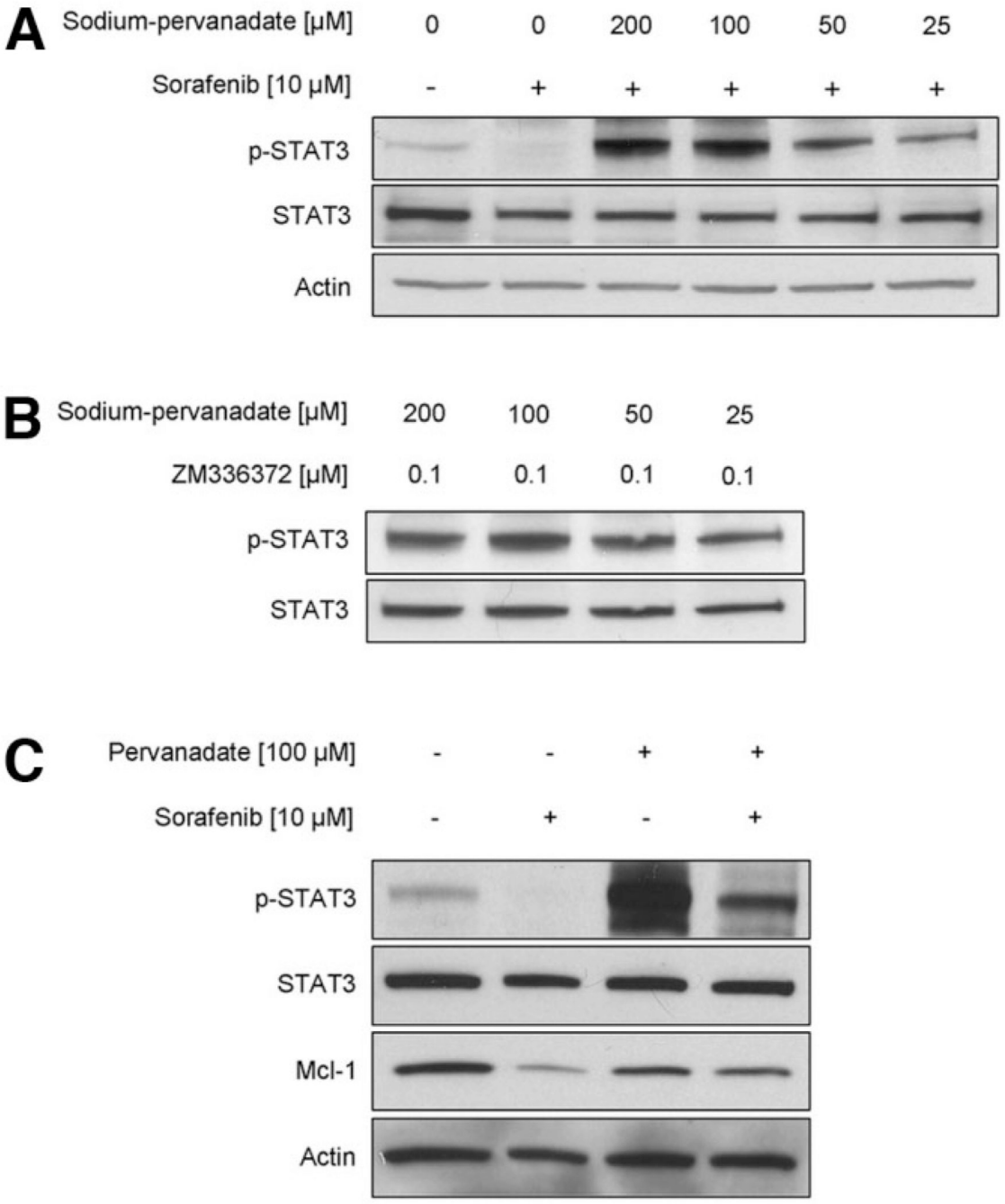

Fig. 3.

Sorafenib-induced Tyr^{705} STAT3 dephosphorylation and Mcl-1 reduction is mediated by Raf-kinase inhibition and depends on phosphatase activity. (A) HuCCT-1 cells were treated with sorafenib (10 μM) in the absence or presence of the phosphatase inhibitor pervanadate at the indicated concentrations. Four hours after treatment, whole-cell lysates were obtained and 50 μg of proteins analyzed by immunoblot analysis for Tyr^{705} phospho-STAT3 and total STAT3. (B) HuCCT-1 cells were cotreated with the b-Raf and c-Raf inhibitor ZM336372 (0.1 μM) and the phosphatase inhibitor pervanadate at the indicated concentrations. Four hours after treatment, whole-cell lysates were obtained and 50 μg of proteins analyzed by immunoblot analysis for Tyr^{705} phosphoSTAT3 and total STAT3. (C) HuCCT-1 cells were cotreated with

sorafenib (10 μM) and the phosphatase inhibitor pervanadate (100 μM). At 12 hours after treatment, whole-cell lysates were obtained and 50 μg protein was analyzed by immunoblot analysis for Tyr^{705} phospho-STAT3, total STAT3, Mcl-1, and actin.

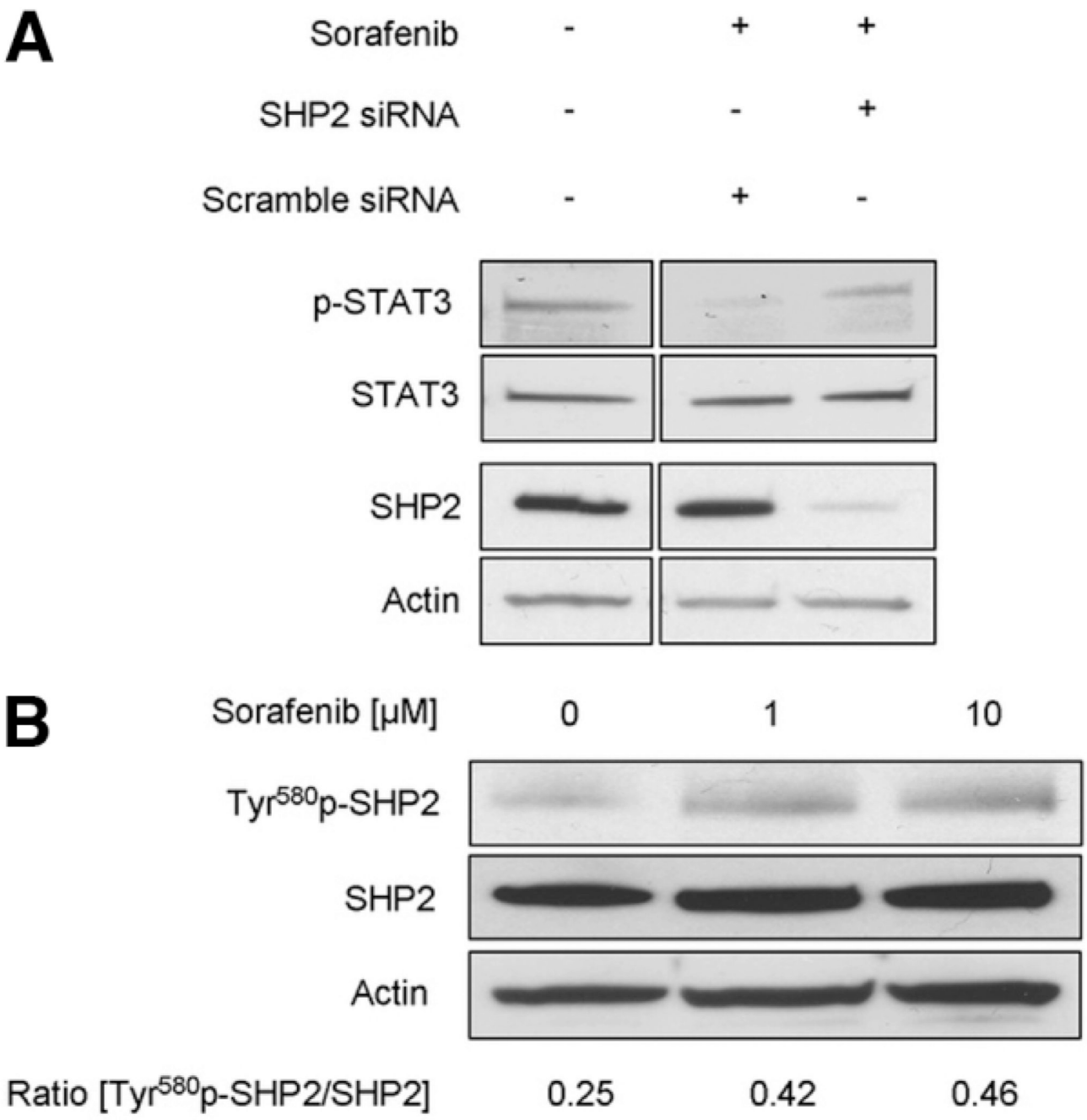

Fig. 4.

Sorafenib-induced Tyr^{705} STAT3 dephosphorylation is mediated by phosphatase SHP2. (A) HuCCT-1 cells were treated for 2 hours with sorafenib at the indicated concentrations followed by immunoblot analysis for Tyr^{580} phospho-SHP2, total STAT3, and actin. The relative increase in Tyr^{580} phospho-SHP2 was quantified by densitometric analysis. (B) HuCCT-1 cells were transfected with scrambled or SHP2-specific siRNA followed by treatment with sorafenib (10 μM) for 4 hours. Subsequently, whole-cell lysates were obtained and 50 μg of proteins analyzed by immunoblot analysis for Tyr^{705} phospho-STAT3, total STAT3 and SHP2. Bands were cut and combined (separated by dotted line) from the same radiograph.

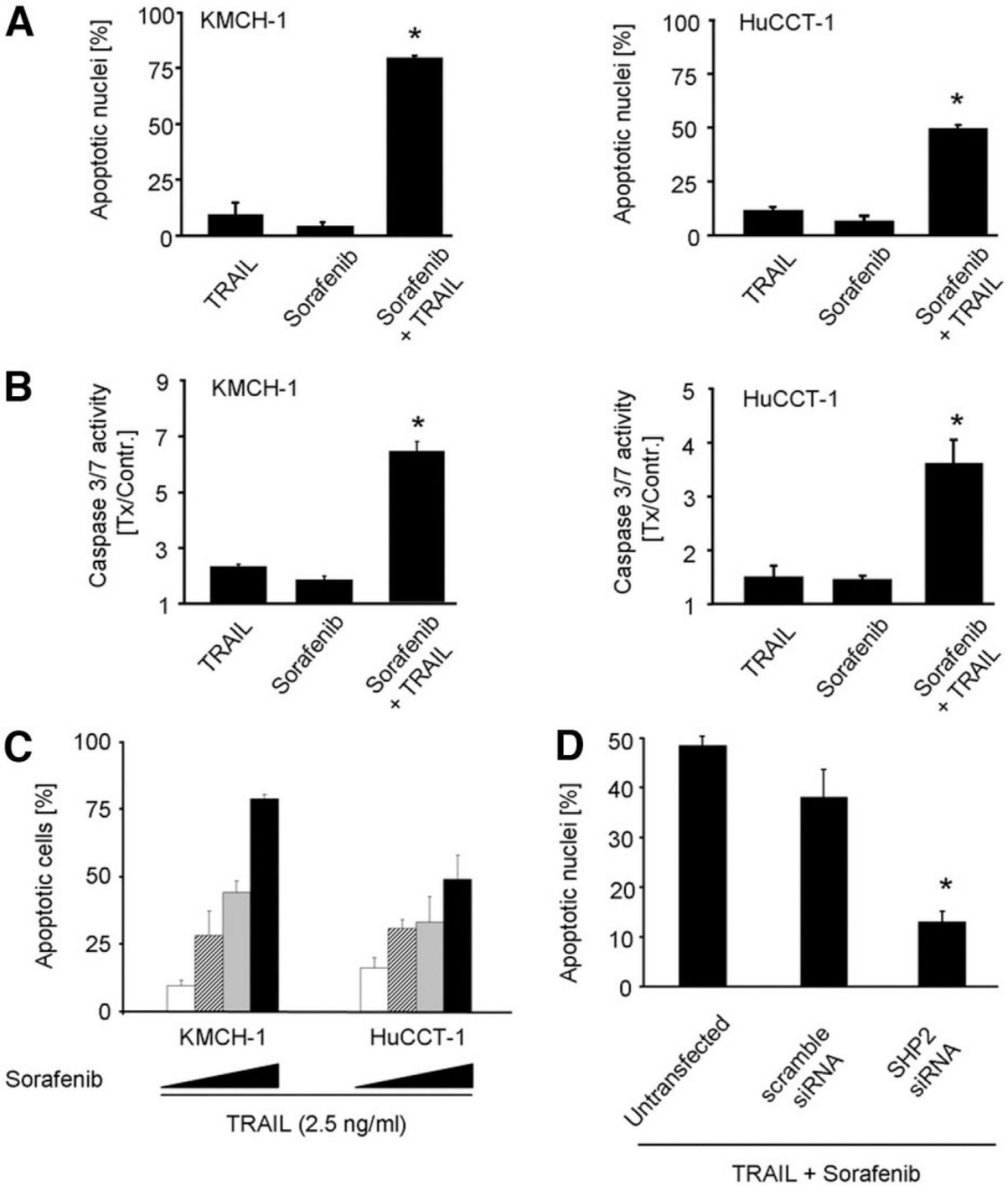

Fig. 5.

Sorafenib sensitizes CCA cells to TRAIL-induced apoptosis. Effects of sorafenib on KMCH-1 (left) and HuCCT-1 cells (right). Shown are average values with standard deviations (n = 3). (A) Cells were treated with sorafenib (10 μM) and/or TRAIL (2.5 ng/mL) followed DAPI-staining and fluorescence microscopic analysis. (B) Cells were treated for 2 hours with sorafenib (10 μM), followed by addition of TRAIL (2.5 ng/mL). Note the significant ($P < 0.05$) increase in caspase 3/7 activity in cells treated with combination treatment. (C) Dose-dependency of sorafenib mediated sensitization to TRAIL-induced apoptosis. HuCCT-1 and KMCH-1 cells were treated with 2.5, 5, and 10 μM of sorafenib in the presence of 2.5 ng/mL TRAIL followed by quantification of apoptotic nuclei using DAPI-staining and fluorescence

microscopic analysis. (D) Untreated, scramble siRNA and SHP2 siRNA transfected HuCCT-1 cells were treated with sorafenib (10 μM) and TRAIL (2.5 ng/mL) followed DAPI-staining and fluorescence microscopic analysis.

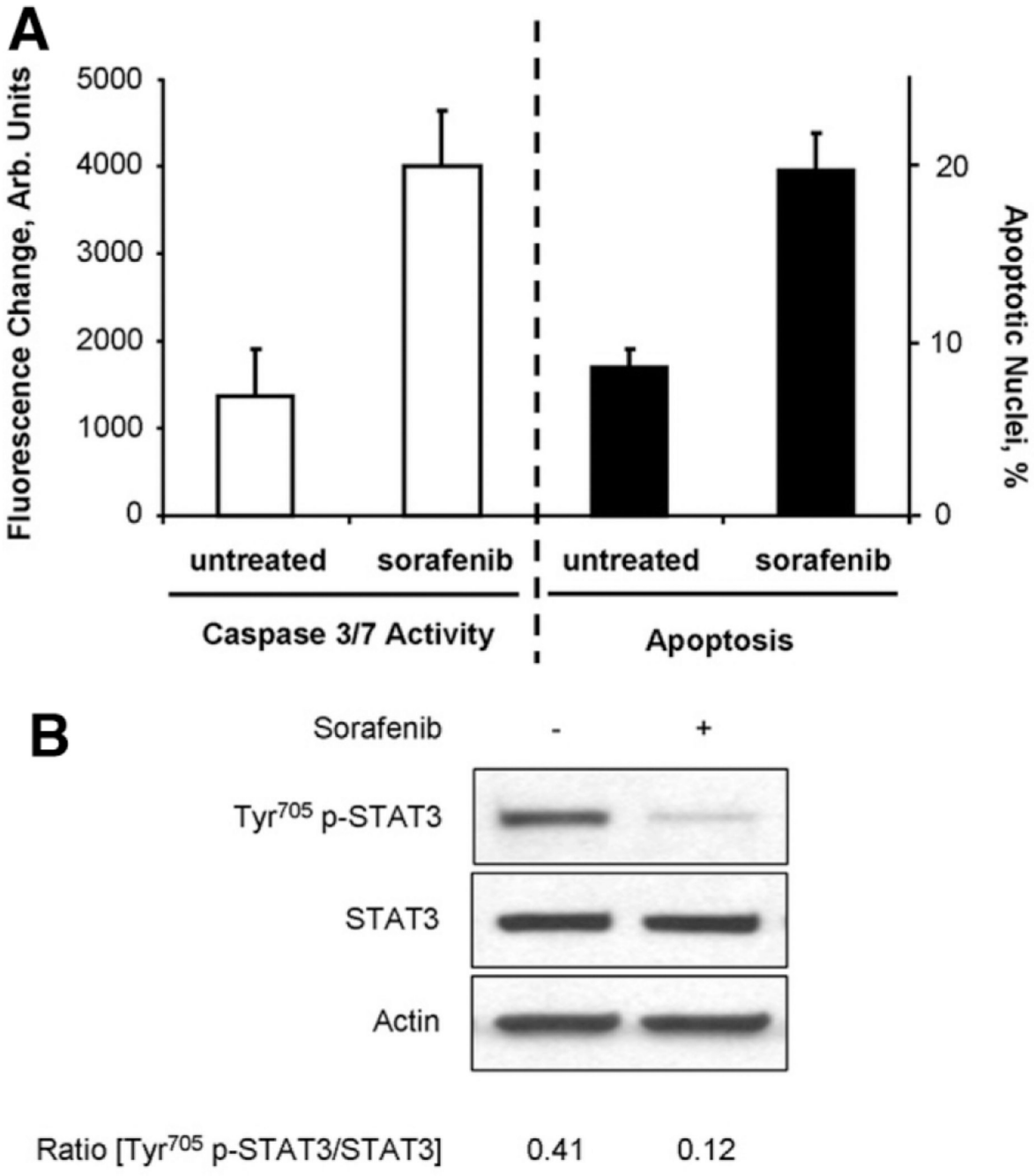

Fig. 6.

Sorafenib monotherapy induces apoptosis in TFK-1 cells. TFK-1 cells were treated for 6 hours in the presence or absence of Sorafenib (10 μM), followed by analysis for apoptosis induction and Tyr^{705} p-STAT3 dephosphorylation. (A) Caspase-3/7 activity (left) and quantification of apoptotic nuclei using DAPI-staining and fluorescence microscopic analysis (right) following sorafenib treatment. (B) Immunoblot analysis for Tyr^{705} phospho-STAT3 and total STAT3 in whole-cell lysates obtained after 6 hours incubation in the presence or absence of sorafenib. The relative decrease in Tyr705 p-STAT3 was quantified by densitometry of three separate experiments.

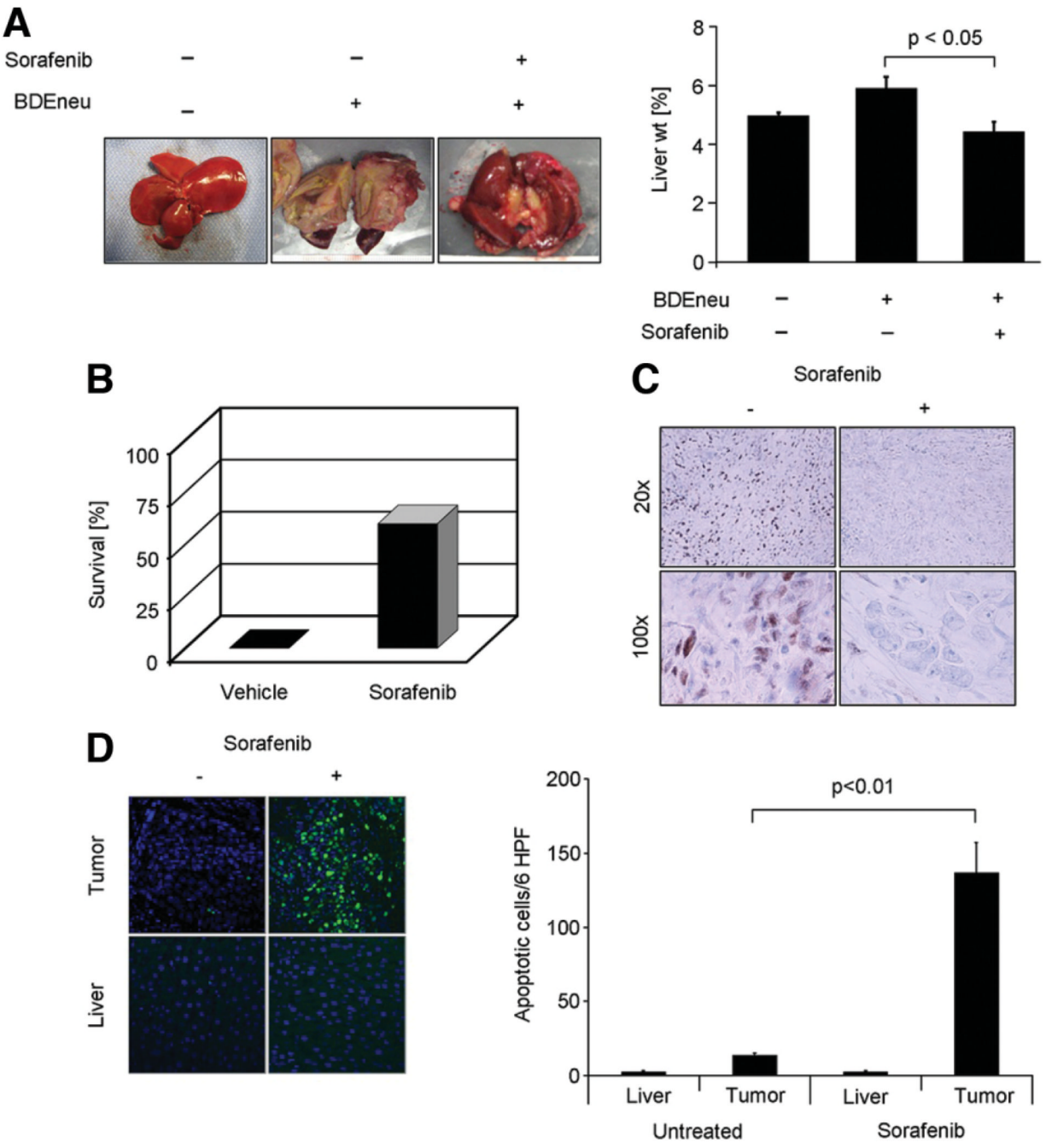

Fig. 7.

Sorafenib is tumor suppressive in a rat, syngeneic, orthotopic rodent model of CCA. BDEneu cells were implanted in left hepatic duct-ligated, male Fischer rats. One week after surgery, animals were treated daily with sorafenib (10 mg/kg body weight) or vehicle by intraperitoneal injection for 7 days (n = 9 animals/treatment group). One week after completion of treatment, all vehicle-treated animals had died, and remaining animals were sacrificed and analyzed. (A) Macroscopic analysis of hepatic tumors. Depicted are photographs of livers of normal, and sorafenib-treated or vehicle-treated tumor-bearing rats. There was almost complete replacement of the liver by tumor tissue in vehicle-treated versus sorafenib-treated animals resulting in significant increase of liver weight in tumor-bearing rats versus normal rats. (B)

Comparison of survival at day 21 after tumor implantation. None of the vehicle-treated animals had survived at day 21 versus 60% animal survival in the sorafenib treatment group. (C) Immunohistochemical analysis for Tyr^{705} phospho-STAT3 in BDEneu tumor-tissue of sorafenib-treated and vehicle-treated rats. (D) TUNEL assay for evaluation and quantification of apoptosis in BDEneu tumor sections of sorafenib-treated and vehicle-treated animals.